

The vibrational line shape of diatomic adsorbates on metal clusters

Estela Blaisten-Barojas^{a)}

Department of Chemistry, The Johns Hopkins University, Baltimore, Maryland 21218

J. W. Gadzuk

National Institute of Standards and Technology, Gaithersburg, Maryland 20899

(Received 6 November 1991; accepted 10 February 1992)

A decrease of at least an order of magnitude in the vibrational relaxation time T_1 has been measured for CO bonded to Rh and Co clusters when the size of the cluster increases from 5 to 35 Å. We propose that this effect is mainly due to the coupling of the molecular vibration ω_0 with the electron-hole excitations in the cluster. This is described via a model Hamiltonian. The finite size of the clusters give rise to a discrete electronic spectrum, and hence to a discrete pair excitation spectrum. This effect is measured in terms of D , the mean spacing between nearest-neighbor levels in the conduction band of the cluster. We find that: (1) the proposed mechanism starts to contribute to T_1 only when $D < \hbar\omega_0$; (2) T_1 is at least several hundred ps for clusters less than 15 Å in size; (3) there is a sharp decrease of T_1 to about 10 ps as the cluster size increases from 15 to 40 Å; (4) T_1 decreases smoothly towards the bulk value for larger clusters.

I. INTRODUCTION

The vibrational properties of chemisorbed molecules on metal surfaces are of importance to phenomena ranging from catalytic chemical reactions to libration mediated absorption. Quantitative determinations of the vibrational relaxation rates from time resolved measurements are now possible.¹⁻³ Molecules chemisorbed on metal surfaces are useful probes of surface chemical dynamics phenomena and speculation about possible molecular relaxation mechanisms has come from theory⁴⁻¹¹ or has been extracted from spectroscopic experiments.¹²⁻¹⁴ It is nevertheless desirable to identify the relevant excitations of the solid (phonons, electron-hole pairs, plasmons) that dissipate and affect any selective localization of energy in a specific chemisorbed molecule or bond. The degree of localization depends on the electronic properties of the surface on which the molecules are adsorbed.^{15,16} If instead of an extended surface the molecules are adsorbed on an atomic cluster or small particle, the degree of localization will also depend on the size of the cluster or particle.¹⁷⁻¹⁹ This issue is the subject matter of this work.

Experimental surface studies by themselves are an interdisciplinary science where chemistry, physics, and engineering get together. Information on how molecules (or atoms) interact with surfaces has been obtained through many new surface spectroscopies.^{16,20} An important connection between the dynamics of molecular vibrations is revealed by the study of spectroscopic line shapes. Assuming that homogeneous broadening can be separated from both inhomogeneous broadening and intermolecular contributions, then the IR absorption line shapes provide information about the interaction mechanisms between the active modes of the adsorbate and the surface excitations. To the extent that homogeneous broadening of vibrational absorption lines can be

attributed to T_1 processes, the main question for molecules adsorbed on metal surfaces concerns the relative importance of phononlike excitations vs electron-hole pairs to account for the observed line widths.^{21,22} The absorption line shape is of the form²³

$$I(\omega) = \frac{1}{2\pi} \lim_{T \rightarrow \infty} \frac{1}{2T} \left\langle \left| \int_0^{2T} q(t) e^{i\omega t} dt \right|^2 \right\rangle, \quad (1)$$

where $q(t)$ is a generalized dynamical coordinate representing the active molecular mode excited at time $t = 0$ in the "spectroscopic event." The loss of temporal self correlation of this vibrational coordinate results in line broadening. This loss can occur via two distinctly different routes. In the first, the decay of the excited vibrational state is due to energy flow either to other molecular modes or to a "bath" of surface modes such as phonons^{24,25} or electron-hole pairs.²¹ This is usually referred to as a T_1 process. In the simplest case when $q(t)$, the molecular mode, is taken as harmonic oscillator,²² this process represents the damping exerted by the medium that results in a decay of the amplitude and therefore the energy of the oscillator.²⁶ Second, if one molecular excited state is populated coherently by a pulse, dephasing can occur in which the correlation of the dynamical variable is lost by elastic collisions with a fluctuating background.²⁷ This process is strongly temperature dependent. It is usually characterized by a time T'_2 indicating the time used by the system to accumulate a real, time dependent phase $\delta(t)$ between $q(t)$ and $q(t' \neq t)$. The energy of the oscillator does not change. With both mechanisms possible, the full width at half-maximum of an absorption line between levels i and f is customarily written as

$$\Gamma = 1/2T_1 + 1/T'_2. \quad (2)$$

Therefore, in order to properly assign a mechanism for the observed homogeneous absorption line width, it is necessary to rely on supplementary experimental data that allows the separation of T_1 from T'_2 contributions to the observed

^{a)} On leave of absence from Instituto de Física, Universidad Nacional Autónoma de México, Ap. Postal 20-364, México 01000 D.F., México.

broadening. Temperature dependence experiments, and real time domain IR pump-probe experiments have recently addressed this point.^{1-3,17-19} It is indeed the current activity in the latter which has provided the motivation for this paper.

In the two-photon experiments, a laser pulse of typically 20 ps in duration is split into pump and probe beams which are focused at a common point on the sample (e.g., diatomics adsorbed on surfaces or clusters).¹⁷⁻¹⁹ The pump pulse defines a time origin $t = 0$ and is used to coherently excite the adsorbate molecules to their first vibrational state $\nu = 1$. The probe beam is delayed a time τ_d and its transmitted intensity is recorded as a function of this time delay. The absorptivity is proportional to the population of the ground state $\nu = 0$. At $t = 0$, the pump produces a population depletion of the ground state, which in turn repopulates exponentially at a rate $\sim 1/T_1$. Thus, measurement of the probe absorptivity as a function of the delay time τ_d provides a time-domain measurement of the vibrational relaxation time T_1 .

These experiments might seem to focus attention on the behavior of the adsorbed molecules and not on the surface. This cannot be so since the adsorbate molecules interact strongly with the surface and, in many cases of catalytic interest, the molecules are generally chemisorbed. In fact, in the pump-probe experiments the energy is placed in the dipole mediated $\nu = 0 \rightarrow \nu = 1$ vibrational excitation of the diatomic adsorbate but can flow to the surface. This transition is the only *active* mode considered as a result of CO having a permanent dipole moment. Other allowed transitions that could be produced by the same laser light might be due to induced dipole moments in the cluster atoms. These transitions are too weak to be detected in the experiment. The overall mechanism is detected by the decrease of population of the $\nu = 1$ excited state; i.e., using a classical terminology, the amplitude of the adsorbate vibrations is effectively reduced due to the molecule-surface interaction. The surface in turn can use this energy to adjust its geometry (surface reconstruction) or open a bond and close another (bond diffusion), or to excite collective motions. In many practical instances, one would like to find systems that are able to store energy in one localized spot for long periods of time (long T_1). This has been observed in certain complexes containing a cluster core of metal atoms. Several carbonyls of transition metal atoms provide an example since the measured T_1 is of the order of $1-2 \times 10^{-10}$ s, implying that the energy deposited in the CO molecules remains localized for thousands of oscillator vibrations.¹⁷⁻¹⁹ However, CO adsorbed on extended metallic surfaces has vibrational relaxation times on the order of a few ps, i.e., almost two orders of magnitude smaller than for the carbonyl molecules. Measurements carried out on CO chemisorbed on transition metal clusters of characteristic size ~ 40 Å supported onto silica surfaces yielded vibrational relaxation times in the range 5-10 ps, times that are of the same order of magnitude as those for an infinite surface.

Therefore, it is relevant to know if there is a critical cluster size at which the relaxation rate is suddenly reduced, and if the change is mainly due to a preferred mechanism. It has been suggested, without further elucidation, that the de-

crease of T_1 when the system is large could be due to electron-hole pair excitations possible in the extended metal but not in smallish carbonyl molecules.^{17,18} The aim of this paper is to provide a rationalization for the reported results. In Sec. II we outline the relevant aspects of the model used to describe the coupling between the localized molecular excitation characterized by $\hbar\omega_0$, the vibrational quantum of energy, and a quasicontinuum of electron-hole pair excitations. The novel premise is based on the finite size quantization of the electronic excitation spectrum in clusters.^{28,29} The theoretical approach is close to Fano's treatment of a discrete state coupled to a continuum,³⁰ with the continuum replaced by a discrete spectrum with variable mean level spacing. Due to the discreteness of the valence band, the electron-hole (eh) pair excitation spectrum presents an energy gap near the Fermi energy. The effect of an energy gap is not present in the Bixon-Jorner model³¹ of intramolecular radiationless transitions which also deals with a localized level coupled to a quasicontinuum. This energy gap in small clusters can be of the order of $\hbar\omega_0$, or even greater. No relaxation is possible in that case and the cluster behaves as insulator-like with respect to vibrational damping. As the cluster grows larger, the energy gap decreases and eventually vanishes for the extended solid. The vanishing energy gap near the Fermi energy, accompanied by the linear increase with energy of the density of eh excitations, make large clusters conductorlike, and thus vibrational relaxation occurs. Therefore, only clusters larger than a critical size exhibit a significant coupling of adsorbate vibrations to electron-hole pairs that makes the vibrational relaxation mechanism feasible. This is quantitatively demonstrated in Secs. III and IV where we present the numerics of our exactly solvable problem applied to CO chemisorbed on Rh clusters. It is found that a sharp change in the trends of the relaxation rate takes place at a cluster size of about 15 Å. The limit of an infinite cluster is in agreement with the Persson and Persson¹² vibrational lifetime estimate for CO on an extended metal surface. Numerical consequences and concluding remarks follow in Sec. V.

II. OSCILLATOR COUPLED TO THE ELECTRON GAS: MODEL HAMILTONIAN

The simplest model suitable for representing a characteristic molecular mode of vibration is that of a localized harmonic oscillator with frequency ω_0 and reduced mass μ . The Hamiltonian can be written in terms of boson operators b, b^\dagger as

$$H_{\text{osc}} = \hbar\omega_0 b^\dagger b, \quad (3)$$

where $q = \sqrt{\hbar/(2\mu\omega_0)}(b^\dagger + b)$, $p = i\sqrt{\hbar\mu\omega_0/2}(b^\dagger - b)$ are the canonical coordinates of the oscillator.

Let us assume that this oscillator is dynamically coupled to the electronic excitations of a finite Fermi system representing a metal cluster. The electronic Hamiltonian involving the N valence electrons in a cluster can be written as

$$H_{\text{elec}} = \sum_s \epsilon_s a_s^\dagger a_s, \quad (4)$$

where, for a finite system without translational symmetry, s can be thought to label the number of nodes of the one-electron wave functions within the volume of the cluster. Then ϵ_s are the single electron eigenvalues giving rise to a discrete valence band, and the operators a_s, a_s^+ satisfy fermion anti-commutation relations. Spin effects will be neglected. The unperturbed zero-temperature ground state of the electron system is then characterized by occupation of the lowest energy $N/2$ one-electron states ϵ_s . The density of available electron states in the entire cluster depends on the number of ions in its core, and therefore on the cluster volume Ω . In a finite system, the Fermi energy is the energy of the highest occupied molecular orbital (HOMO). This molecular orbital can be a complicated combination of core ion orbitals, and usually it is nondegenerate with the lowest unoccupied molecular orbital (LUMO). The energy gap between the HOMO and the LUMO is an important quantity relevant to quantum-size effects. For metals, the HOMO-LUMO energy difference falls off to zero as the cluster grows larger.

In order to quantify these finite-size effects and follow a process as a function of increasing cluster size, a helpful rule of thumb is to watch for the changes of the mean energy between first-nearest-neighbor states in the valence band (D). For a small cluster D is large, but $D \rightarrow 0$ as the cluster size increases to become an extended solid. On the average, the number of available electron states in the valence band is $2/D$. Therefore, *per unit volume of cluster*, there are $1/(D\Omega)$ cells with unitary volume Ω_0 . Assuming that each cell contains one metal atom, a cluster with $n = \Omega/\Omega_0$ core ions has a density of available electron states per atom

$$g(D) = 2/(Dn). \quad (5)$$

Now suppose that at the Fermi energy, $g(\epsilon_F)$ is a constant regardless of cluster size. The limit of large n and small D needs to be taken *simultaneously* as indicated in Eq. (5).

The interacting system, localized molecular oscillator coupled to the electronic excitations of the cluster, can be expressed as

$$H = H_{\text{osc}} + H_{\text{elec}} + H_{\text{int}}. \quad (6)$$

With respect to the interaction Hamiltonian we consider the following facts. First, low energy excited states of the Fermi system can be represented by electron-hole pair operators

$$\tilde{\rho}_{ss'}^+ = a_{s+s'}^+ a_s \quad (7)$$

indicating that a *hole* is created in a single-electron state s below the Fermi level and an *electron* is created in state $s + s'$ above the Fermi level.²¹ The electronic configurations corresponding to these low energy monoexcitations $\tilde{\hbar}\omega_{ss'}^0 = (\epsilon_{s'} - \epsilon_s)$ characterize the fluctuations of the total electron density about the mean electron density obtained from the single electron description of the ground state. The density fluctuations can be formally cast in terms of creation (and annihilation) operators in the random phase approximation (RPA) as

$$\rho_{s'}^+ = \sum_s a_{s+s'}^+ a_s = \sum_s \tilde{\rho}_{ss'}^+, \quad (8)$$

where the summation runs only on single electron states s which are occupied in the ground state. Therefore, a density

fluctuation operator indexed s' represents a coherent superposition of electron-hole pairs (or electronic configurations arising from monoexcitations of the ground state). Second, the simplest coupling between scalar fields is an operator linear in both localized oscillator displacements and electron density fluctuations (breakdown of the Born-Oppenheimer approximation) that can be written as

$$H_{\text{int}} = \frac{\hbar}{\sqrt{2}} \sum_s \lambda_s (\rho_{s'}^+ + \rho_s) (b^+ + b). \quad (9)$$

Here λ_s are the coupling constants between the internal molecular coordinate and the metal core represented by many sets of electron-hole excitations labeled s . Units of frequency were chosen for λ_s . The virtue of the model Hamiltonian given in Eq. (6), which is a result of adding Eqs. (3), (4), and (9), is that it possesses an exact solution for finite systems within the RPA.

It is convenient to introduce new operators to describe the dynamics behind the interaction Hamiltonian, namely,

$$A_{ss'}^+ \equiv \tilde{\rho}_{ss'}^+ + \tilde{\rho}_{ss'} \quad \text{and} \quad B = 1/\sqrt{2}(b^+ + b). \quad (10)$$

The equations of motion thereby obtained are

$$\ddot{A}_{ss'}^+ + (\omega_{ss'}^0)^2 A_{ss'} = -2\lambda_s \omega_{ss'}^0 B \quad (11a)$$

and

$$\ddot{B} + \omega_0^2 B = -\omega_0 \sum_{s,s'}' \lambda_s A_{ss'}^+, \quad (11b)$$

where the prime indicates summation over occupied levels s (below or at the Fermi energy) to virtual levels s' above the Fermi energy. Close inspection of these coupled differential equations reveals a similarity to the equations of motion of a set of coupled harmonic oscillators. In our case one oscillator of frequency ω_0 (molecule) is coupled to a finite quasi-continuum of oscillators of frequencies $\omega_{ss'}^0$ (electron-hole pair bath). The set of differential equations can be transformed into a set of coupled algebraic equations by writing the operators in Eqs. (11) as linear combinations of normal modes of oscillation of frequencies ω_ℓ (Ref. 32)

$$A_{ss'}^+(t) = \sum_\ell \xi_{ss',\ell} e^{i\omega_\ell t},$$

$$B(t) = \sum_\ell \xi_{0,\ell} e^{i\omega_\ell t}, \quad (12)$$

where ℓ is a running index counting all the possible monoexcitations $s \rightarrow s'$. The set of equations in Eqs. (11) is thus reduced to a solvable eigenvalue problem

$$\|\mathbf{M} - \omega^2 \mathbf{1}\| \xi = 0. \quad (13)$$

Here ξ is the vector formed by the coefficients in Eqs. (12) and \mathbf{M} is a sparse matrix³³ called "arrow-head matrix"³⁴

$$\mathbf{M} = \begin{pmatrix} \omega_0^2 & \tilde{\lambda}_1 & \tilde{\lambda}_2 & \tilde{\lambda}_3 & \tilde{\lambda}_4 & \dots \\ \tilde{\lambda}_1 & (\omega_1^0)^2 & 0 & 0 & 0 & \dots \\ \tilde{\lambda}_2 & 0 & (\omega_2^0)^2 & 0 & 0 & \dots \\ \tilde{\lambda}_3 & 0 & 0 & (\omega_3^0)^2 & 0 & \dots \\ \tilde{\lambda}_4 & 0 & 0 & 0 & (\omega_4^0)^2 & \dots \end{pmatrix}, \quad (14)$$

where $\tilde{\lambda}_l = \sqrt{2\omega_0\omega_l^0}\lambda_l$. The determinant of the matrix given by Eq. (13), when equated to zero, gives the formal implicit equation for the squared eigenfrequencies

$$\omega_l^2 - \omega_0^2 = \sum_{s,s'} \frac{2\omega_0\omega_{ss'}^0|\lambda_{s'}|^2}{\omega_l^2 - (\omega_{ss'}^0)^2}. \quad (15)$$

The coefficients $\xi_{0,l}$ and $\xi_{ss',l}$ in Eq. (12) are

$$\xi_{0,l}(\omega_l^2 - \omega_0^2) = \omega_0 \sum_{s,s'} \lambda_{s'} \xi_{ss',l} \quad (16)$$

and

$$\xi_{ss',l} = 2\lambda_s \omega_{ss'}^0 \xi_{0,l} / (\omega_l^2 - (\omega_{ss'}^0)^2). \quad (17a)$$

These coefficients are normalized, such that

$$|\xi_{0,l}|^2 + \sum_{s,s'} |\xi_{ss',l}|^2 = 1. \quad (17b)$$

Using Eqs. (15)–(17) one is able to obtain the closed expression

$$|\xi_{0,l}|^2 = \left[1 + 4 \sum_{s,s'} \frac{|\lambda_{s'}|^2 (\omega_{ss'}^0)^2}{[\omega_l^2 - (\omega_{ss'}^0)^2]^2} \right]^{-1}. \quad (18)$$

The formulation described above for treating a localized molecular oscillator coupled to electron-hole pair modes representing the excited states of a metal cluster closely resembles the Bixon–Jortner model for radiationless transitions.³¹ In contrast to the analytic solutions of that simplified model, however, we can generate precise numerical solutions of Eq. (13) that give a more realistic picture of the effect of a discrete bath of excitations on the decay of one excited molecular vibration level (in this case $\nu = 1$).

The absorption spectrum for the IR-active mode is obtained from Eqs. (1), (12), and (18)

$$I(\omega) = \frac{2\pi\hbar}{\mu\omega_0} \sum_l |\xi_{0,l}|^2 \delta(\omega - \omega_l). \quad (19)$$

Therefore, the line shape function is a sum of delta functions placed at the eigenfrequencies ω_l which are the solutions of the eigenvalue Eq. (13). The heights of these delta functions are determined by $|\xi_{0,l}|^2$ as given in Eq. (18). This “envelope function” specifies the relative absorption of energy that each normal mode undertakes from the IR photon.

III. THE INFRARED LINE SHAPE AS A FUNCTION OF CLUSTER SIZE

Clusters made out of atoms in the first two series of transition metals have one or two electrons in the 4s or 5s subshell and a partially filled inner 3d or 4d subshell. When such atoms are brought together to make, first a cluster, then a microcrystal, and finally an extended solid, overlap of the s states is very strong but overlap of states from the unfilled inner d state is rather weak. The density of states of the valence band that builds up as the cluster grows larger has two ingredients. The d block of levels (or band) extends only over a moderate range of energy but has a very large density of states over this range. This band overlaps in energy with the s band resulting in a fractional electron per atom occupancy of the s band due to d to s conversion. The fewer, highly mobile electrons in the s band do most of the work of

conduction in such a metal, but it is the large density of states of the d band at the Fermi energy which controls properties such as the electronic specific heat and magnetic properties. It is also this large density of states that proves important in our problem of vibrational relaxation.

In order to simulate the quasicontinuum of excitations represented by Eq. (4) two possible strategies can be adopted. In the first, a geometry of the cluster atoms is assumed *a priori* and the one-electron states giving rise to the discrete valence band are calculated within an approximation of the all electron Schrödinger equation. It is generally accepted that clusters may adopt unique structures far different from pieces cut out of lattice models. In the investigation of the size dependence of a cluster property, the valence band of the cluster needs to be calculated for every cluster size and/or for every cluster geometry considered. This strategy might never cover all the possibilities. The second approach is to generate the valence band of the cluster (or superposition of bands near the Fermi energy) *a priori* by following a statistical treatment based on electronic spectrum fluctuations.^{35,36} This scenario emphasizes the discreteness of the valence band via the mean first-nearest-neighbor level spacing D , which defines locally the band mean density of states as $2/D$.³⁷ The one-electron levels giving rise to the band in consideration are subsequently generated *numerically* from a preselected statistical distribution of first-nearest-neighbor level spacings consistent with D . The specifics of the distributions reveal the symmetries of the Hamiltonian. We adopt this second strategy.

The simplest jellium model for clusters is the spherical well model, whose electronic spectrum fluctuations satisfy a Poisson distribution of first-nearest-neighbor level spacings S (Ref. 38)

$$P(S) = (1/D) \exp(-S/D). \quad (20)$$

This statistics causes the levels to cluster together such that small first-nearest-neighbor level spacings are more abundant. The reason for assuming level clustering, or lack of repulsion, is that the discrete spectrum under consideration is a superposition of several pure spectra³⁵ (sequences of levels with same values of angular momentum quantum numbers) all derived from the same total cluster Hamiltonian. One can then assume that very delocalized electrons (strong overlap between valence electrons) in a cluster might be well represented by Poisson statistics.

On the other hand, at least in two examples of clusters with fairly localized electrons (poor overlap at interatomic distances beyond first neighboring atoms), the electronic spectrum fluctuations of the valence d band of a nickel cluster calculated in the linear combination of atomic orbitals method (LCAO) tight binding approximation, and the molecular levels of an organometallic complex obtained in the Hartree–Fock approximation were also shown to follow Poisson statistics.³⁹ In these cases neither the model or solution approximation considered contained interactions among the fermions sufficient to produce significant repulsion between every other pair of levels.

The opposite situation to Poisson statistics is a uniform distribution, in which all single particle levels are equally

spaced by D . From the electronic spectrum fluctuations scenario the spectrum generated with a uniform distribution is a picket fence, presents the maximum repulsion or *rigidity*. Because of its simplicity the uniform distribution is usually encountered in theoretical approximations,³¹ although only the harmonic oscillator presents such a spectrum. Analysis of sequences of levels in relevant systems might satisfy other statistics—e.g., Gaussian orthogonal ensemble, symplectic, or unitary.^{36,37,40} These statistics give rise to spectra with a degree of rigidity intermediate between Poisson (no rigidity) and uniform distributions (maximum rigidity). Therefore for the purposes of this work, we consider only the two extreme cases, namely, Poisson and uniform distributions.

Instead of taking into account the complete valence band, we consider a block of levels that extends over the energy range $\epsilon_F - (\hbar\omega_0 + 2D)$ to $\epsilon_F + (\hbar\omega_0 + 2D)$. Energy levels outside this range give rise to eh pair excitations which are too high in energy when compared to the molecular vibrational energy $\hbar\omega_0$. Couplings λ_s between the molecular mode and those eh excitations arising between levels outside the chosen energy window are assumed to be negligible. The active block of levels gives rise to a half filled band of one-electron levels. The Hamiltonian representing the bound electrons within this band is given by Eq. (4). We call this block of levels the *excitation band* and assume that: (i) the block contains cluster states that resulted from linear combinations of the outermost d and s states of the cluster atoms (eventually also p states), and (ii) the density of single electron states is constant in the region where the excitation band extends, but depends on cluster size as $2/D$. We generate the excitation band numerically either from the uniform or the Poisson distributions.

Low energy eh pairs originate as a result of monoexcitations from levels below the Fermi level ϵ_F to levels above it. These excitations give rise to non-negligible couplings and they are all within the excitation band. Each monoexcitation requires a certain energy $\hbar\omega_{ss'}^0 = (\epsilon_{s'} - \epsilon_s)$ to create a hole in an occupied state ϵ_s below ϵ_F and an electron in a virtual state $\epsilon_{s'}$ above ϵ_F . In what follows, we will use one running index ℓ to label, in increasing order, the energy differences characteristic of each eh pair. The distribution of nearest-neighbor eh pair frequencies follows the same statistics as the spectrum of one-electron levels from which the eh pairs were generated. It is either uniform or Poisson. In both cases the number of eh pair excitations of energy $\hbar\omega$ per unit of energy is the same, and is given by

$$\rho(\omega) = \sum_{\ell} \delta(\omega - \omega_{\ell}) = \frac{\omega}{D^2}. \quad (21)$$

This relation is valid as long as the density of states of the one-electron levels is almost constant. In the case of a free electron gas, Eq. (21) holds well up to energies of the order $\epsilon_F/2$ (Ref. 41). Equation (21) shows that the degeneracy of the electron-hole pair excitations increases linearly with energy. The low-energy behavior of $\rho(\omega)$ plays a crucial role in the effects considered here. In fact, for finite systems ω cannot be zero. Therefore, the density of eh excitations presents a size-dependent gap between zero and the energy of the first possible monoexcitation. This gap is nothing else but the

energy between the HOMO and LUMO states which is of the order of D . The gap disappears as the system grows to become an extended solid.

The elements are now given to solve numerically the eigenvalue problem in Eq. (13) and obtain the set of eigenstates of the coupled system. It is convenient to adopt reduced units of ω_0 for eh frequencies and coupling constants λ_{ℓ} . We assume: (i) that all coupling constants are equal to Λ within a frequency window $\omega_0 - 1.5D \leq \omega \leq \omega_0 + 1.5D$ but zero otherwise, (ii) that within this frequency window the coupling constant scales as $\Lambda^2/D = \text{const} \tan t$ and, (iii) that within the frequency window of interest $\rho(\omega) = \rho(\omega_0)$. The number of *active* eh pair excitations is $3/D$, which we consider as smoothly distributed over the span of the frequency window. For each value of D , the unperturbed eh frequencies ω_{ℓ}^0 are generated numerically for both the uniform and the Poisson distributions. It is this group of ω_{ℓ}^0 that we bring into the eigenvalue equation, Eq. (13). The resulting eigenfrequencies ω_{ℓ} are subsequently carried into Eq. (18) to obtain the envelope function and thus the IR line shape function $I(\omega)$.

The Rh-CO system discussed in the introduction provides an excellent example of the interactions at work. We generate numerically the eh band of rhodium carbonyls with metallic clusters of various sizes by assigning values to the pertinent constants: $\omega_0 = (2\pi c) \times 2200 \text{ cm}^{-1}$ (c is the speed of light) (Ref. 18), $g(\epsilon_F) = 1.37 \text{ states/eV atom}$ mainly due to d states,⁴² and $\Omega_0 = 30.3 \text{ \AA}^3$ consistent with an atomic radius of 1.34 \AA . The best fit to the very scarce experimental data (three points)^{17,18} yielded $\Lambda^2/D = 3.03 \times 10^{-7} \omega_0$ as the proper scaling for the interaction constant.

In Figs. 1 and 2 we show the line shapes as a function of cluster size obtained for the uniform and Poisson spectra, respectively. In the plots, each Dirac delta function in Eq. (19) has been depicted by a spike as narrow as the width of the available drawing line. One spike is positioned on the frequency scale at each eigenfrequency obtained from Eq. (13). The height of the spikes is given by the coefficients calculated from Eq. (18). When the metal cluster is very small the apparent absorption band is made up by one delta function centered near ω_0 , all other lines being too weak to make any contribution to the bandwidth. This is shown in Figs. 1(a) and 2(a) for the case of the Rh carbonyls, where the plot is for a cluster having 170 atoms within a sphere of 15 \AA in diameter. For this cluster size range $D > 35 \text{ cm}^{-1}$. As clusters grow larger, a qualitative change in the band shape is observed. The band near ω_0 is now composed of several lines, and the number of spikes with noticeable heights increases with cluster size, as shown in Figs. 1(b) through 1(d) and Figs. 2(b) through 2(d). The absorption band for clusters with less than 20 \AA in diameter [Figs. 1(b), 1(c), and 2(b), 2(c)] have a structure that could be observed if enough experimental resolution were available.

As the cluster increases in size, the spacing between spikes shrinks dramatically. It is on the order of one tenth of a wave number for 20 \AA clusters [Figs. 1(c) and 2(c)], and decreases to one hundredth of wave number for clusters in the 25 \AA size range [Figs. 1(d)–1(f) and 2(d)–2(f)]. This ef-

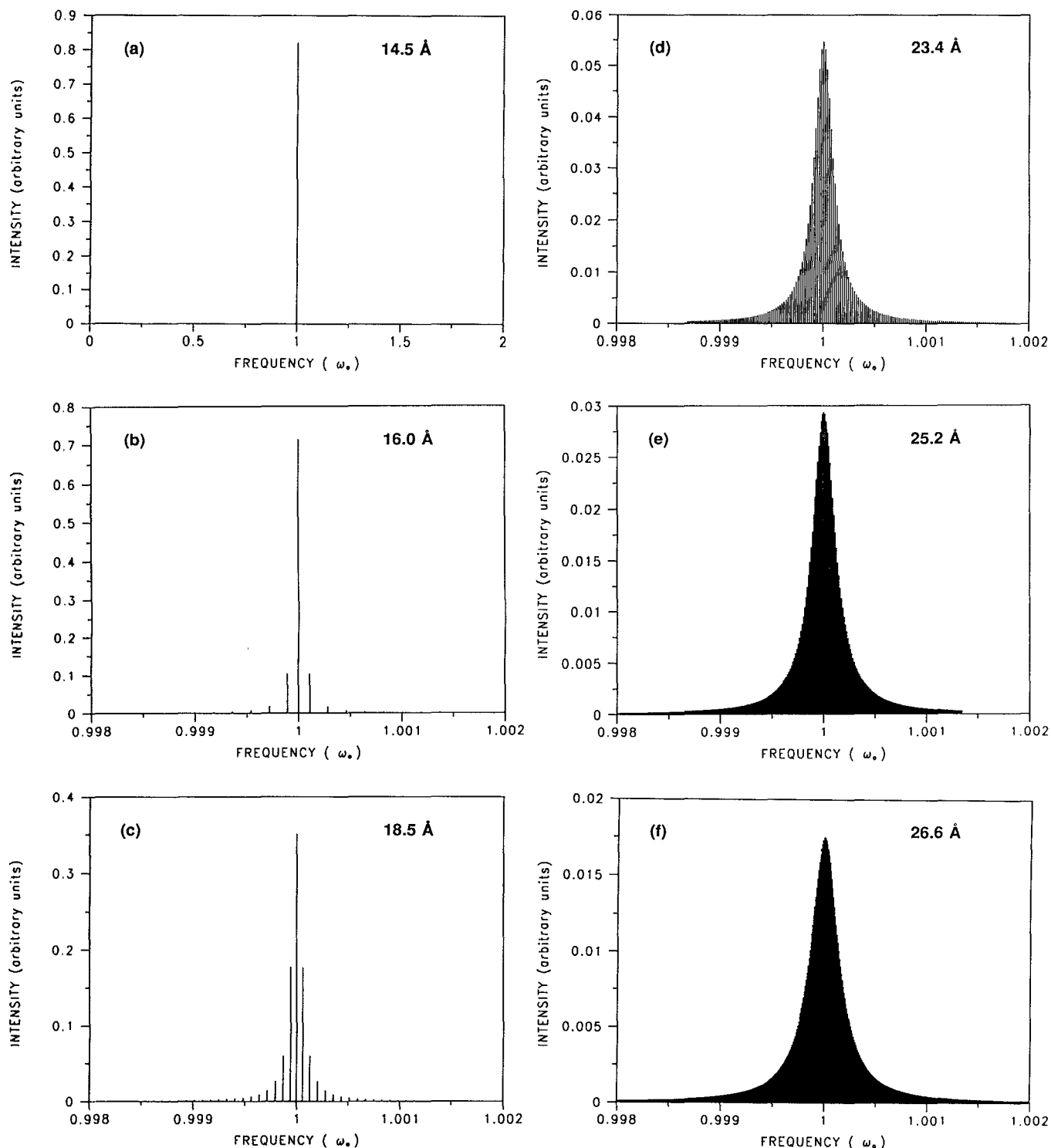


FIG. 1. Calculated absorption bands as a function of cluster size using the uniform distribution of one-electron levels. Data corresponds to CO adsorbed on Rh clusters with increasing diameter: (a) 14.5 Å; (b) 16 Å; (c) 18.5 Å; (d) 23.4 Å; (e) 25.2 Å; (f) 26.6 Å. Frequency is given in units of $\omega_0 = (2\pi c) \times 2200 \text{ cm}^{-1}$.

fect is made obvious from the increasing “darkening” of the bands. Indeed, the number of delta functions making up these bands increases linearly with the number of atoms in the metal cluster. Atomic vibrations and librations in condensed phases give rise to line widths comparable to these spacings. Therefore, for clusters in the 25 Å size range, the

experimentalist detects the envelope of the band centered at ω_0 . The band envelope is clearly bell shaped in the case of the uniform distribution of ω_i^0 's [Figs. 1(b)–1(f)] allowing to measure the band broadening directly from the width at half maximum height. In the case of the Poisson distribution of ω_i^0 's, the bands present more structured shapes [Figs. 2(b)–

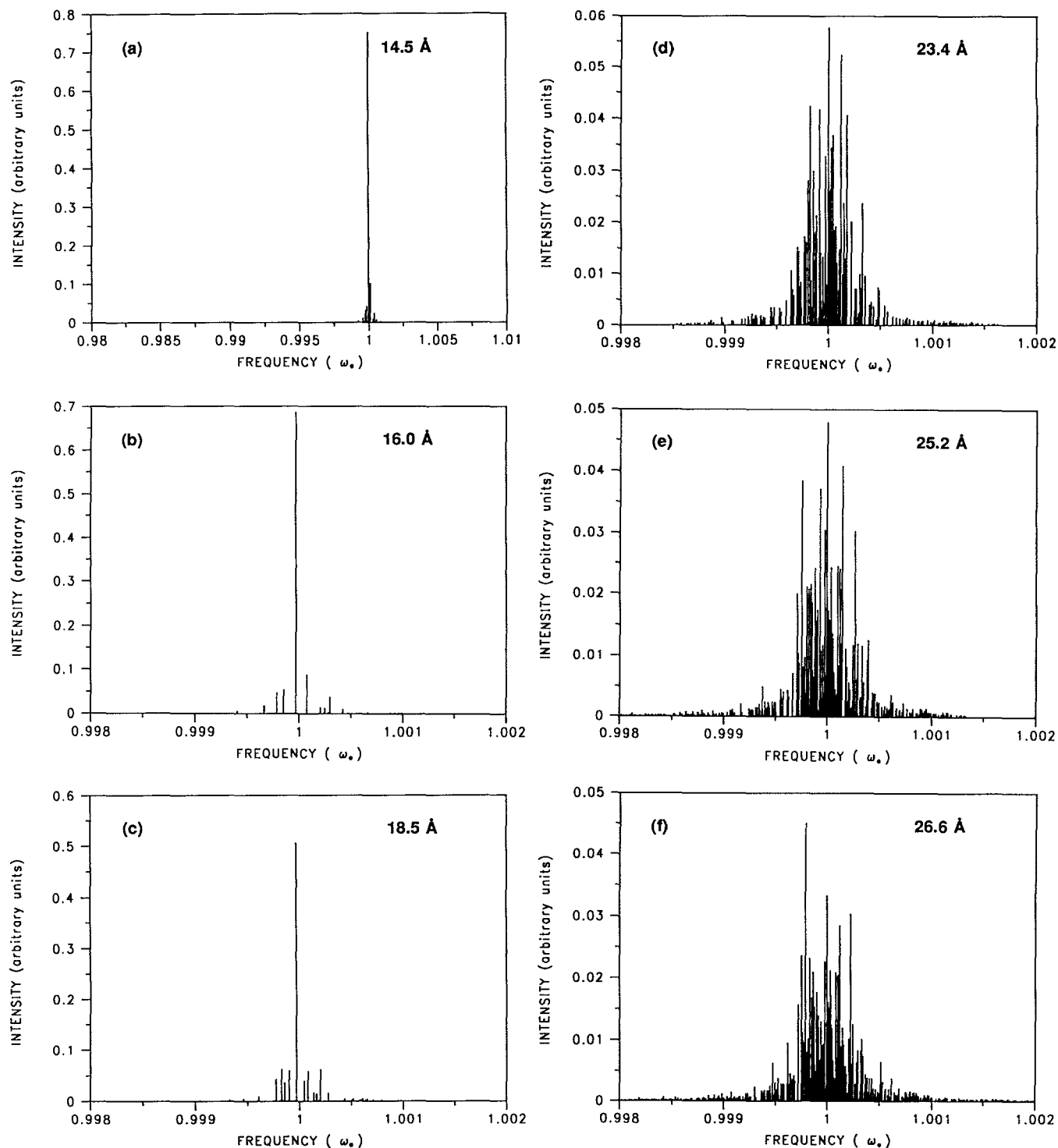


FIG. 2. Calculated absorption bands as a function of cluster size using the Poisson distribution of one-electron levels. Data corresponds to CO adsorbed on Rh clusters with increasing diameter: (a) 14.5 Å; (b) 16 Å; (c) 18.5 Å; (d) 23.4 Å; (e) 25.2 Å; (f) 26.6 Å. Frequency is given in units of $\omega_* = (2\pi c) \times 2200 \text{ cm}^{-1}$.

2(f)] showing that the absence of regularity in the electronic spectrum affects both the position of the spikes and the band shape. The structured appearance of the bands in the Poisson case is due to randomness in the coefficients weighting the delta functions in Eq. (19). We emphasize that the average number of delta functions building up the bands in both,

Fig. 1 and Fig. 2, is the same for clusters of equal size. No attempt to smooth such shapes was done while plotting Fig. 2. However, bands were smoothed to evaluate their broadening by giving a Gaussian width to the delta functions composing each band. The half-maximum widths of the Poisson bands, calculated from their smoothed envelope, change

with cluster size just as much as the widths obtained using the uniform distribution. This is discussed in Sec. IV.

IV. METAL/NONMETAL TRANSITION AS A QUANTUM SIZE EFFECT

Let us characterize the band broadening Γ by the width at half-height of the calculated band centered at ω_0 . Within our precision, the bandwidths are the same for bands originated with a uniform or Poisson distribution. In Fig. 3 we have collected these widths obtained from calculations corresponding to Rh-CO with metallic cores of various sizes. The data show the abrupt change of the broadening per atom as a function of cluster size. It is very clear that the metal core in the carbonyl compounds have two very distinct behaviors. Below approximately 25 Å in diameter the metal core in the carbonyl compounds shows *nonmetallic* behavior. Above 25 Å in diameter the electron hole mechanism produces a substantial line broadening—the metal core of the compound clusters behaves as a *metal*. This defines a critical size N_c . From the above results we can extrapolate that the mechanism of broadening due to excitation of electron-hole pairs probed by the chemisorbed carbonyls has an effective range, which is on the order of 25 Å for the system Rh-CO or $N_c \sim 1000$ atoms. Therefore, this type of systems can be probed by changes on the vibrational relaxation of the adsorbates as a function of the metallic core size. We can state that clusters with more than N_c behave already as metallic surfaces, or alternatively, that the extended metallic surface can be modeled by clusters in this size range, at least with respect to vibrational line shape spectroscopy. This metal-nonmetal behavior is a *quantum size effect* revealed by the discreteness of the spectrum.

The bulk limit is readily obtained from Eq. (15). It gives rise to the usual complex frequency solution

$$\omega^2 = \omega_0^2 + \omega_0(\Delta + i\Gamma), \quad (22)$$

where Δ is the self energy responsible for shifts,

$$\Delta = PP \sum_{s,s'}' \frac{2\omega_{ss'}^0 |\lambda_{s'}^0|^2}{\omega_s^2 - (\omega_{ss'}^0)^2} \quad (23)$$

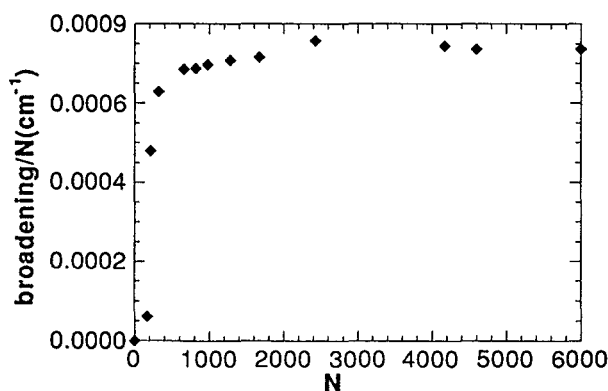


FIG. 3. Broadening per atom as a function of the number of atoms in the metallic cluster. Data corresponds to the calculation using the uniform distribution of one electron levels.

and where PP is the principal part and Γ is the imaginary part that accounts for the absorption in the system

$$\Gamma = 2\pi \sum_{s,s'}' |\lambda_{s'}^0|^2 \omega_{ss'}^0 \delta(\omega^2 - (\omega_{ss'}^0)^2). \quad (24)$$

Since in most cases Δ and Γ are slowly varying functions of frequency, one can replace them by their value at ω_0 . Then, the line shape function in the continuous limit is a Lorentzian

$$I(\omega) = \frac{\omega}{2\pi} \frac{\omega_0 \Gamma(\omega_0)}{[\omega^2 - \omega_0^2 + \omega_0 \Delta(\omega)]^2 + [\omega_0 \Gamma(\omega_0)]^2}. \quad (25)$$

Replacing the summation by an integral, taking into account the density of eh pairs, Eq. (21), one obtains for the broadening function per atom

$$\Gamma(\omega_0) = \pi(\Lambda^2/D)g(\omega_F)\omega_0. \quad (26)$$

Furthermore, when values of the constants are specified in Eq. (26), the limiting value for large sizes shown in Fig. 3 is obtained. Since we have addressed only one mechanism of relaxation, it is possible to define the relaxation time T_1 from the broadening as

$$T_1 = 1/(2\Gamma N), \quad \text{for } N < N_c \\ = 1/(2\Gamma N_c), \quad \text{for } N > N_c. \quad (27)$$

The calculated data for Γ , shown in Fig. 3, and Eq. (27) allow to fit T_1 by an analytical expression such that the relaxation time as a function of the number of atoms in the metal core is

$$T_1 = A(B + K(N_c/N - 1)\exp[\alpha(N_c/N - 1)]), \quad (28)$$

where the values of the constants are $A = 15$ ps, $B = 1.5$, $K = 0.609$, $\alpha = 0.171$, and $N_c = 1420$. The limit for large N gives $T_1 = A(B - Ke^{-\alpha}) = 14.8$ ps. Although the suggested expression for the fit gives a plausible size dependence and evidences the critical size, it is by no means a unique fit. The limiting value for the infinite surface has not been measured for Rh-CO yet, but it is 2 ps for Pt-CO (Ref. 18) and 4 ps for Cu-CO (Ref. 13). The order of magnitude is correct.

V. CONCLUSION

Electron-hole pair excitations understood as a representation of the fluctuations of the electron density in the metallic core of carbonyls, coupled to the internal vibrations of adsorbed molecules, are shown to provide a mechanism for energy dissipation leading to dramatic changes in the CO vibrational relaxation time as a function of the metallic core size. The size dependence is made evident through the discreteness of the one-electron spectrum of the metallic cluster core which allows for the transformation of the equations of motion of the density operators Eqs. (11a) and (11b) into the finite set of algebraic equations cast in Eq. (13). This eigenvalue equation is solved numerically in two different limits of the one-electron spectrum: (i) rigid spectrum generated from a uniform distribution of energy levels; and (ii) Poisson spectrum indicating the absence of level repulsion. The eigenvalue problem is solved under an ansatz for the coupling between electronic and nuclear motions that (i)

assumes all coupling constants λ_{ν} to have a constant value Λ in a narrow window of energy with width D around $\hbar\omega_0$ and zero otherwise; (ii) scales the value of Λ as $\Lambda^2/D = \text{const} \tan t$; (iii) keeps the density of electron-hole pair excitations constant within the narrow window of non-zero interactions.

The example of rhodium carbonyls is worked out in full. It is shown very clearly that energy dissipation due to the eh mechanism starts to be effective when the metal cluster core of the carbonyl compound is large enough, i.e., on the order of 15 Å. Up to this characteristic size, the small clusters behave as nonmetallic. For them the CO vibrational relaxation time is very long, on the order of several hundred picoseconds. However, the transition to a metallic behavior is fairly sharp as the size is further increased because clusters in the 25 Å size range attain already the vibrational relaxation time of the infinite surface. The later is on the order of 10 ps.

Therefore, we have been able to show that a nonmetallic/metallic transition can be identified in transition metal carbonyls by probing the behavior of the vibrational relaxation time of the adsorbates as a function of the size of the metallic core. We encourage further measurements to confirm this prediction.

ACKNOWLEDGMENTS

E. B. B. acknowledges support by the National Science Foundation (Grant No. RII-8902850) and the hospitality of the Surface Science Division of the National Institute of Standards and Technology where part of this work was carried out.

- ¹ J. D. Beckerle, M. P. Casassa, R. R. Cavanagh, E. J. Heilweil, and J. C. Stephenson, *Phys. Rev. Lett.* **64**, 2090 (1990).
- ² E. J. Heilweil, R. R. Cavanagh, and J. C. Stephenson, *J. Chem. Phys.* **84**, 2361 (1986).
- ³ E. J. Heilweil, J. C. Stephenson, and R. R. Cavanagh, *J. Phys. Chem.* **92**, 6099 (1988).
- ⁴ B. N. J. Persson, *J. Phys. C* **17**, 4741 (1984).
- ⁵ A. G. Eguiluz, *Phys. Rev. B* **30**, 4366 (1984).
- ⁶ B. I. Lundqvist, in *Many-Body Phenomena at Surfaces*, edited by D. C. Langreth and H. Suhl (Academic, Orlando, 1984), p. 453.
- ⁷ J. W. Gadzuk and A. C. Luntz, *Surf. Sci.* **144**, 429 (1984).
- ⁸ D. C. Langreth, *Phys. Rev. Lett.* **54**, 126 (1985).

- ⁹ R. G. Tobin, *Surf. Sci.* **183**, 226 (1987).
- ¹⁰ H. Ueba, *Prog. Surf. Sci.* **22**, 181 (1986).
- ¹¹ D. C. Langreth, *Physica Scripta* **35**, 185 (1987).
- ¹² B. N. J. Persson and M. Persson, *Solid State Commun.* **36**, 175 (1980); B. N. J. Persson and R. Ryberg, *Phys. Rev. Lett.* **48**, 549 (1982).
- ¹³ R. Ryberg, *Phys. Rev. B* **32**, 2671 (1985).
- ¹⁴ Y. J. Chabal, *Phys. Rev. Lett.* **55**, 845 (1985).
- ¹⁵ R. Hoffmann, *Rev. Mod. Phys.* **60**, 601 (1988).
- ¹⁶ J. W. Gadzuk, in *Vibrational Spectroscopy of Molecules on Surfaces*, edited by J. T. Yates and T. E. Madey (Plenum, New York, 1987), p. 49 and references therein.
- ¹⁷ E. J. Heilweil, R. R. Cavanagh, and J. C. Stephenson, *J. Chem. Phys.* **89**, 5342 (1988).
- ¹⁸ J. D. Beckerle, M. P. Casassa, R. R. Cavanagh, E. J. Heilweil, and J. C. Stephenson, *J. Chem. Phys.* **90**, 4619 (1989); J. D. Beckerle et al., *ibid.* **95**, 5403 (1991).
- ¹⁹ E. J. Heilweil, M. P. Casassa, R. R. Cavanagh, and J. C. Stephenson, *Annu. Rev. Phys. Chem.* **40**, 143 (1989).
- ²⁰ *Vibrations at Surfaces*, edited by D. A. King, N. V. Richardson, and S. Holloway (Elsevier, Amsterdam, 1986); A. M. Bradshaw and H. Conrad, Editors, *ibid.* (1987); Y. T. Chabal, F. M. Huffman, and G. P. Williams, *ibid.* (1990).
- ²¹ J. W. Gadzuk, *Phys. Rev. B* **24**, 1651 (1981).
- ²² P. Avouris and B. N. J. Persson, *J. Phys. Chem.* **88**, 837 (1984).
- ²³ M. L. Koszykowski, D. W. Noid, and R. A. Marcus, *J. Phys. Chem.* **86**, 2113 (1982).
- ²⁴ E. Blaisten-Barojas and M. Allavena, *J. Phys. C* **9**, 3121 (1976).
- ²⁵ I. L. Garzon and E. Blaisten-Barojas, *J. Chem. Phys.* **83**, 4311 (1985).
- ²⁶ E. J. Heller, *Acc. Chem. Res.* **14**, 368 (1981).
- ²⁷ R. M. Shelby, C. B. Harris, and P. A. Cornelius, *J. Chem. Phys.* **70**, 34 (1979).
- ²⁸ D. M. Wood and N. W. Ashcroft, *Phys. Rev. B* **25**, 6255 (1982).
- ²⁹ W. P. Halperin, *Rev. Mod. Phys.* **58**, 536 (1986).
- ³⁰ U. Fano, *Phys. Rev.* **124**, 1866 (1961).
- ³¹ M. Bixon and J. Jortner, *J. Chem. Phys.* **48**, 715 (1968).
- ³² G. D. Mahan, *Many Particle Physics* (Plenum, New York, 1981).
- ³³ R. P. Tewarson, in *Large Sparse Sets of Linear Equations*, edited by J. K. Reid (Academic, London and New York, 1971), p. 151.
- ³⁴ D. P. O'Leary and G. W. Stewart (private communication).
- ³⁵ C. E. Porter and N. Rosenzweig, in *Statistical Theories of Spectra: Fluctuations*, edited by C. E. Porter (Academic, New York, 1965), p. 234.
- ³⁶ T. A. Brody, J. Flores, J. B. French, P. A. Mello, A. Pandey, and S. S. M. Wong, *Rev. Mod. Phys.* **53**, 385 (1981).
- ³⁷ J. Barojas, E. Blaisten-Barojas, J. Flores, and E. Cota, *KINAM* **1**, 361 (1979).
- ³⁸ J. Barojas, E. Cota, E. Blaisten-Barojas, and J. Flores, *Ann. of Phys.* **107**, 95 (1977).
- ³⁹ J. Barojas, E. Blaisten-Barojas, and J. Flores, *Phys. Lett. A* **69**, 142 (1978).
- ⁴⁰ S. L. Coy and K. K. Lehmann, *Phys. Rev. A* **36**, 404 (1987).
- ⁴¹ E. Muller-Hartman, T. V. Ramakrishnan, and G. Toulouse, *Phys. Rev. B* **3**, 1102 (1971).
- ⁴² D. A. Papaconstantopoulos, *Handbook of the Band Structure of Elemental Solids* (Plenum, New York, 1986), p. 154.